Protonation of Glu L212 following Q_B^- Formation in the Photosynthetic Reaction Center of *Rhodobacter sphaeroides*: Evidence from Time-Resolved Infrared Spectroscopy†

R. Hienerwadel,‡,⊥ S. Grzybek,‡,§ C. Fogel,‡ W. Kreutz,‡ M. Y. Okamura,|| M. L. Paddock,|| J. Breton,⊥ E. Nabedryk,⊥ and W. Mäntele*,‡,§

Institut für Biophysik und Strahlenbiologie, Universität Freiburg, Albertstrasse 23, 79104 Freiburg, Germany, Department of Physics, University of California, San Diego, La Jolla, California 92093-0319, and SBE/DBCM, CEN Saclay, 91191 Gif-sur-Yvette Cédex, France

Received May 3, 1994; Revised Manuscript Received October 18, 1994⊗

ABSTRACT: The protonation events that occur upon $Q_A^-Q_B \rightarrow Q_AQ_B^-$ electron transfer in photosynthetic reaction centers from *Rhodobacter sphaeroides* were investigated by time-resolved infrared spectroscopy using tunable diode lasers as previously described [Mäntele, W., Hienerwadel, R., Lenz, F., Riedel, E. J., Grisar, R., & Tacke, M. (1990) *Spectrosc. Int. 2*, 29−35; Hienerwadel, R., Thibodeau, D. L., Lenz, F., Nabedryk, E., Breton, J., Kreutz, W., & Mäntele, W. (1992) *Biochemistry 31*, 5799−5808]. In the mid-infrared region between 1695 and 1780 cm^{-1}, transient signals associated with $Q_A^-Q_B \rightarrow Q_AQ_B^-$ electron transfer were observed and characterized. The dominant transient absorbance changes are three positive signals at 1732, 1725, and 1706 cm^{-1} and two negative signals at 1716 and at 1698 cm^{-1}. The 1725 cm^{-1}-signal disappears upon $^1H \rightarrow ^2H$ exchange as expected for an accessible COOH group and is absent in Glu L212 Gln mutant reaction centers. On this basis, we propose an assignment of this signal to the COOH group of Glu L212. The other signals could correspond to intensity changes and/or shifts of other carboxylic residues, although contributions from ester C=O groups of bacteriopheophytins cannot be ruled out. In native reaction centers at pH 7 and at 4 °C, biphasic kinetics of the transient components were observed at most frequencies. The major signal at 1725 cm^{-1} exhibits a fast kinetic component of $t_{1/2}$ = 0.18 ms (25% of the total amplitude) and a slow one of $t_{1/2}$ = 1 ms (75% of the total amplitude). A global fit analysis of the signals between 1695 and 1780 cm^{-1} revealed that the spectral distributions of the fast and the slow components are different. Biphasic kinetics with comparable half-times were also observed for the Glu L212 to Gln mutant. The simplest model to explain these results is that the fast phase represents electron transfer and the slow phase represents proton transfer and/or conformational changes coupled to electron transfer. The difference spectra of the slow component from native reaction centers show that the 1725 cm^{-1} band corresponds to an absorbance increase and not to a shift of an existing band. The signal is therefore proposed to arise from the protonation of Glu L212. The amplitude of the 1725 cm^{-1} signal varies distinctly with pH as expected for protonation of a COO^- group. With increasing pH, the amplitude of the slow component increases while that of the fast component decreases slightly. Both components slow down with increasing pH reaching half-times of 0.3 and 2.5 ms, respectively, at pH 10. These results can be explained if one assumes that Glu L212 is partly protonated upon single-electron reduction of Q_B. On the basis of integrated extinction coefficients of COOH residues, a proton uptake of 0.3−0.6 H^+ at pH 7 per reaction center by Glu L212 is proposed. This proton uptake shows little variation from pH 5 to pH 9 but increases above pH 9. This behavior cannot be explained by the titration of a single isolated titrating residue. However, it can be interpreted by the interaction of Glu L212 with other charged groups in the Q_B site.

The bacterial photosynthetic reaction center (RC)[1] is the membrane protein that initiates the transformation of light energy into chemical energy by coupling light-induced electron transfer to proton uptake associated with the two-electron reduction of the secondary quinone Q_B:

$$2e^- + 2H^+ + Q_B \rightarrow Q_BH_2 \quad (1)$$

This proton uptake is the first step in the proton pump that couples electron transfer to proton transfer across the membrane and drives ATP synthesis [reviewed in Cramer and Knaff (1990)]. The question of the pathway and

† Funding by NIH Grant GM 41637 to M.Y.O. and by the EC Science program (SC 100335) to W.M. and J.B. is gratefully acknowledged. W.M. is grateful for continuous funding by the Deutsche Forschungsgemeinschaft through several grants and a Heisenberg fellowship.

* Author for correspondence: telephone, 49-9131-85-7317(7319); fax, 49-9131-85-8307; e-mail, maentele@pctc.chemie.uni-erlangen.de.

‡ Universität Freiburg.

§ Present address: Institut für Physikalische und Theoretische Chemie, Universität Erlangen-Nürnberg, Egerlandstrasse 3, 91058 Erlangen, Germany.

|| University of California, San Diego.

⊥ CEN Saclay.

⊗ Abstract published in *Advance ACS Abstracts,* February 1, 1995.

[1] Abbreviations: RC, reaction center; D, primary electron donor; Q_A and Q_B, primary and secondary electron acceptor quinones, respectively; Q-10, ubiquinone-10; $k_{AB}^{(1)}$, $k_{AB}^{(2)}$, k_{AD}, and k_{BD}, rates of electron transfer from Q_A to Q_B for the first (1) and second (2) electron and recombination rates from Q_A and Q_B to D, respectively.

0006-2960/95/0434-2832$09.00/0

mechanism of proton transport from aqueous solution to Q_B arises since the X-ray crystal structure of the RC of *Rhodopseudomonas viridis* (Deisenhofer et al., 1984) and *Rhodobacter (Rb.) sphaeroides* (Allen et al., 1986, 1987; Chang et al., 1986; El-Kabbani et al., 1991) revealed that Q_B is buried within the protein out of contact with bulk water and suggested a number of protonatable amino acid side chain residues that could be responsible for proton transfer to reduced Q_B. The role of some of these residues has been probed by site-directed mutagenesis (Paddock et al., 1989, 1990a,b, 1994a; Takahashi & Wraight, 1990, 1992). Mutations of protonatable residues to non-protonatable residues at some sites (such as Ser L223 and Asp L213) block (i.e., slow down rates by 2−3 orders of magnitude) both electron and proton transfer, whereas a mutation at another site (Glu L212) blocks only proton transfer [for a review, see Okamura and Feher (1992)]. The mechanism for the reduction of Q_B involves two one-electron steps with rate constants $k_{AB}^{(1)}$ and $k_{AB}^{(2)}$:

$$Q_A^- Q_B \xrightarrow{k_{AB}^{(1)}} Q_A Q_B^- \quad (2)$$

$$2H^+ + Q_A^- Q_B^- \xrightarrow{k_{AB}^{(2)}} Q_A Q_B H_2 \quad (3)$$

The singly reduced Q_B^- formed by transfer of the first electron in reaction 2 was shown to be in the unprotonated anionic semiquinone state by optical (Verméglio, 1977; Wraight, 1977) and ENDOR (Feher et al., 1985) spectroscopy. However, proton uptake accompanying Q_B^- formation occurs due to proton uptake by acid groups whose pK_a values are increased due to interaction with the negative charge on Q_B^- (McPherson et al., 1988; Maroti & Wraight, 1988). Several acidic residues including Glu L212, Asp L213, and Asp L210 near Q_B have been shown by site-directed mutagenesis to affect rates of electron transfer to Q_B. Most notably, the mutation of Glu L212 to Gln was found to eliminate the pH dependence of $k_{AB}^{(1)}$ and of k_{BD}, the recombination reaction $D^+Q_B^- \rightarrow DQ_B$ (k_{BD}), which both have inflection points near pH 9.5 (Paddock et al., 1989; Takahashi & Wraight, 1992). These changes were interpreted by a simple model in which Glu L212 has a pK_a of 9.5, which is increased upon Q_B^- formation. Consequently, Glu L212 should be involved in proton uptake only at high pH (above 9.5).

Infrared (IR) spectroscopy should be a powerful technique to analyze proton transfer reactions in the RC, since it can directly monitor vibrational modes from amino acid side chains that are sensitive to protonation/deprotonation reactions. This application of IR spectroscopy has been extensively demonstrated in the bacteriorhodopsin field [for a recent review, cf. Rothschild (1992)]. In previous investigations, light-induced Fourier transform infrared (FTIR) difference spectroscopy has been used to analyze the changes in the vibrational spectrum of the RC upon $D^+Q_A^-/DQ_A$ or $D^+Q_B^-/DQ_B$ charge separation (Mäntele et al., 1985; Bagley et al., 1990; Nabedryk et al., 1990) or upon the intermediary electron acceptor reduction (Nabedryk et al., 1986). In a different approach, electrochemically-induced FTIR techniques have been applied to analyze the changes of the vibrational spectrum occuring upon oxidation (D^+/D) of the donor side (Leonhard & Mäntele, 1993). All these difference spectra exhibit highly structured bands resulting from alterations to individual bonds in the RC, predominantly of the cofactors involved, without any evidence for large domains of the protein being affected.

Recently, several FTIR techniques have been employed to identify the changes in the vibrational spectrum of the RC due to quinone (Q_A or Q_B) reduction. These investigations include steady-state Fourier transform infrared (FTIR) $Q_A \rightarrow Q_A^-$ or $Q_B \rightarrow Q_B^-$ difference spectra (Mäntele et al., 1990a, Breton et al., 1991a,b, 1994; Bauscher et al., 1993) and kinetic as well as steady-state $Q_A^-Q_B \rightarrow Q_AQ_B^-$ double difference spectra (Thibodeau et al., 1990, 1992; Buchanan et al., 1992). A number of bands were observed, including vibrational bands of protein residues perturbed by quinone reduction. The strongest signals are observed in the peptide C=O range (amide I, ca. 1700−1630 cm^{-1}), the range of the amide II and the aromatic amino acid side chain modes (approximately 1560−1510 cm^{-1}), and the range between 1500 and 1450 cm^{-1}, where the C−O and C−C modes of the semiquinone anion appear (Bauscher et al., 1990; Bauscher & Mäntele, 1992, Breton et al., 1992a). Q_A^-/Q_A or Q_B^-/Q_B FTIR difference spectra, however, also show signals in the 1700−1750 cm^{-1} range, where absorption bands of carboxylic groups, i.e., of Asp and Glu side chains, are present (Venyaminov & Kalnin, 1990). Since no contributions from the quinone molecule itself are expected [the highest frequency mode of the ubiquinone in vitro in the 2000−1000 cm^{-1} range is the C=O peaking at 1670−1630 cm^{-1}; cf. Bauscher and Mäntele (1992)], the signals in this region can be attributed to molecular changes in the protein induced by quinone reduction.

While steady-state FTIR Q_A^-/Q_A or Q_B^-/Q_B difference spectra reflect the molecular processes at the acceptor side of the RC in the respective relaxed states, recent microsecond to second time-resolved IR spectroscopy using tunable IR diode lasers (Mäntele et al., 1990b) has shown IR signals due to $Q_A^-Q_B \rightarrow Q_AQ_B^-$ electron transfer with 120−150 μs half-time (at 4 °C) (Hienerwadel et al., 1992a). In addition to those changes which reflect either bands characteristic for the formation of the Q_B^- state or decay of the Q_A^- state, slower absorption changes in the millisecond range were detected at 1617 cm^{-1} (attributed to the disappearance of a COO^- mode) and at several frequencies above 1700 cm^{-1} (attributed to the appearance of COOH modes). In preliminary investigations on mutant RC, the lack of a positive band at 1728 cm^{-1} in FTIR difference spectra and the lack of a millisecond transient at 1725 cm^{-1} in kinetic IR signals for the Glu L212 to Gln mutant were taken as evidence for (partial) uptake of a proton by Glu L212 upon formation of Q_B^- (Hienerwadel et al., 1992b). Although proton uptake by Glu L212 seems to be in conflict with the model in which the pK_a of Glu L212 is approximately 9.5 (Paddock et al., 1989; Takahashi & Wraight, 1990), it would be consistent with a model that includes interactions between titrating residues (Beroza et al., 1991; Gunner & Honig, 1992).

The spectral region between approx. 1695 and 1780 cm^{-1} covers the major range for carboxylic C=O modes. In this range, protonation of an Asp or Glu residue ($R\text{-}COO^- + H^+ \rightarrow R\text{-}COOH$) would lead to a positive signal from the appearance of the C=O bond. Correspondingly, a negative signal would appear upon deprotonation ($R\text{-}COOH \rightarrow R\text{-}COO^- + H^+$). A pair of positive and negative bands could correspond to a proton transfer between two groups; however, the shift of the C=O mode due to a change of H-bonding or

of the environment could also lead to a differential signal. In model compound spectra, Asp and Glu C=O modes show molar extinction coefficients of 280 and 220 L mol^{-1} cm^{-1}, respectively (Venyaminov & Kalnin, 1990). If similar extinction coefficients are assumed in RC, protonation and deprotonation of an Asp/Glu side chain should thus give rise to IR signals corresponding to at most $10^{-4}-10^{-3}$ of the IR absorbance (typical set to 1 at the amide-I band). In addition, signals in this range might also arise from shifts of ester or keto C=O vibrations of the bacteriopheophytins as a consequence of the electrostatic field of the negative charge on Q_A^- or Q_B^- (Mäntele et al., 1990a; Breton et al., 1992a). The different origins of IR absorbance changes could well lead to a complex overlap of several signals and thus necessitate a complete temporal and spectral analysis of the transients in this spectral range for a clear assignment.

Here, we present time-resolved IR and steady-state FTIR signals for native RCs in ^1H_2O and ^2H_2O and the mutant Glu L212 to Gln, which in conjunction with the analysis of the pH dependence can be interpreted as proton uptake by Glu L212 upon formation of Q_B^-. We propose from these data a model for charge rearrangement at ionizable groups in the Q_B site that leads to a favorable electrostatic environment for Q_B^-.

MATERIALS AND METHODS

Sample Preparation. Reaction centers from *Rb. sphaeroides* R26 were prepared as previously described (Paddock et al., 1990a). RCs without Q_B were prepared as described by Okamura et al. (1975). For IR sample preparation, RCs were transferred to a buffer containing 100 mM KCl. Succinate buffer (pH range 5−5.5), MES buffer (pH range 5.8−6.5), TRIS buffer pH range 7−8), borate buffer (pH range 9−9.5), and CAPS buffer (pH 10) were used at 100 mM concentrations. With the preadjusted pH, RCs were concentrated to approximately 0.5−1 mM using Centricon and Microcon (Amicon, Witten) ultrafiltration cells with a 30-kDa exclusion limit. A sample of approximately 5 μL of the concentrated RC was transferred to the demountable IR microcell described by Hienerwadel et al. (1992a) and further reduced in water content by a gentle stream of N_2 to a volume of approximately 1−2 μL. In case of incomplete occupancy of the Q_B site, excess ubiquinone (Q_{10}) was added in hexane as described by Breton et al. (1991b). Infrared samples were prepared for a minimum transmission of 30% in the 1690−1760 cm^{-1} range to optimize signal amplitudes.

Deuteration of RC was performed by suspending RC in ^2H_2O buffers of the same composition as described above and equilibrating for 16 h at 15 °C before concentrating to 0.5−1 mM. The degree of $^1H/^2H$ exchange in the liquid phase of the RC sample was estimated >90% by comparison of the O−^{1}H and O−^{2}H stretching vibrations for a sample made to be fully transparent in the mid-IR and somewhat smaller for the protein as estimated from the relative intensities of the amide-II protein band in ^1H_2O and ^2H_2O.

The site-directed replacement of Glu L212 with Gln was previously described (Paddock et al., 1989). RCs were isolated from semiaerobically grown cells so as to not select for functional revertants as described.

Spectroscopy. Time-resolved IR signals (μs to s) were recorded with the kinetic IR photometer using tunable IR diode lasers as described by Mäntele et al. (1990b) and Hienerwadel et al. (1992a). The laser modes used for the experiments described here range from approximately 1695 to approximately 1780 cm^{-1} and were spaced 4−5 cm^{-1}. As an additional feature, a computer-controlled sample wheel carrying up to 10 thermostated samples developed by us was used. The samples were sequentially exposed to the IR measuring beam and the exciting laser flash (595 nm, 15 ns, ca. 5 mJ) allowing a longer time to dark-adapt between flashes. Transient IR signals were recorded by automated selection of a sample recording and compensation of the transmitted IR light (I_0) at a specified IR wavelength and storing the corresponding flash-induced signal in a transient recorder. Series of different pH and with $^1H-^2H$ substitution were performed with a set of different samples in the sample wheel, alternately averaging the kinetic traces in respective files in the transient recorder. This guaranteed that signals from different samples were recorded at precisely the same IR laser mode structures. For the data shown, only laser monomodes were used. The temperature was 4 °C.

IR and UV/VIS/NIR absorbance spectra of the samples were recorded using a combined spectrophotometer described previously (Mäntele, 1993). Time-resolved NIR absorbance changes at 960 nm (rise and decay of the D^+ band) and at 760 nm [shift of the bacteriopheophytin band, cf. Verméglio and Clayton (1977)] were recorded using a setup consisting of near-IR light-emitting diode (LED) sources, appropriate interference filters, and a photodiode detector with a rise time of approximately 200 ns. FTIR spectra of Q_B photoreduction were obtained as described by Breton et al. (1991b) and Hienerwadel et al. (1992b).

Data Analysis. A global fit analysis of an entire set of kinetic traces between 1695 and 1780 cm^{-1} for each sample was performed after the baselines ($I_{t<0}$) had been set to zero and calculation of the absorbance change from ΔI and I_0 had been performed. For the fitting procedure, the strong, instantaneously appearing absorbance change arising from $D^+Q_A^-$ formation (see below in Results) were suppressed by interactively subtracting the 1780 cm^{-1} signal from all other signals in such a way that the resulting amplitude at $t = 5$ μs was zero. The signals above 1780 cm^{-1} have been recently attributed to an electronic transition within D^+ (Breton et al., 1992b). This procedure thus formally corresponds to subtraction of a $D^+Q_A^-/DQ_A$ difference spectrum and additionally ensures that no contributions of $D^+Q_A^- \rightarrow DQ_A$ recombination are present within the transient signals, especially at such frequencies where strong contributions of D^+/D and only small contributions from the acceptor sites are present. As an example for the presentation of the data, Figure 1 will show raw, uncorrected absorbance transients, while Figure 2 will show three-dimensional representations of the transient signals with the contributions from D^+/D removed.

Different samples were normalized using the instantaneous absorbance increase at 1780 cm^{-1} as an internal standard, which has been attributed to an electronic transition within D^+ (Breton et al., 1992b). The Mexfit program (Müller et al., 1991) was used for the global fit analysis with minor modifications for data input and output. Weighting of data points [for details, see Müller et al. (1991)] was done using the standard deviation of the pre-trigger baseline. The Grafit fitting routine was used for the fitting of signals at individual wavelengths.

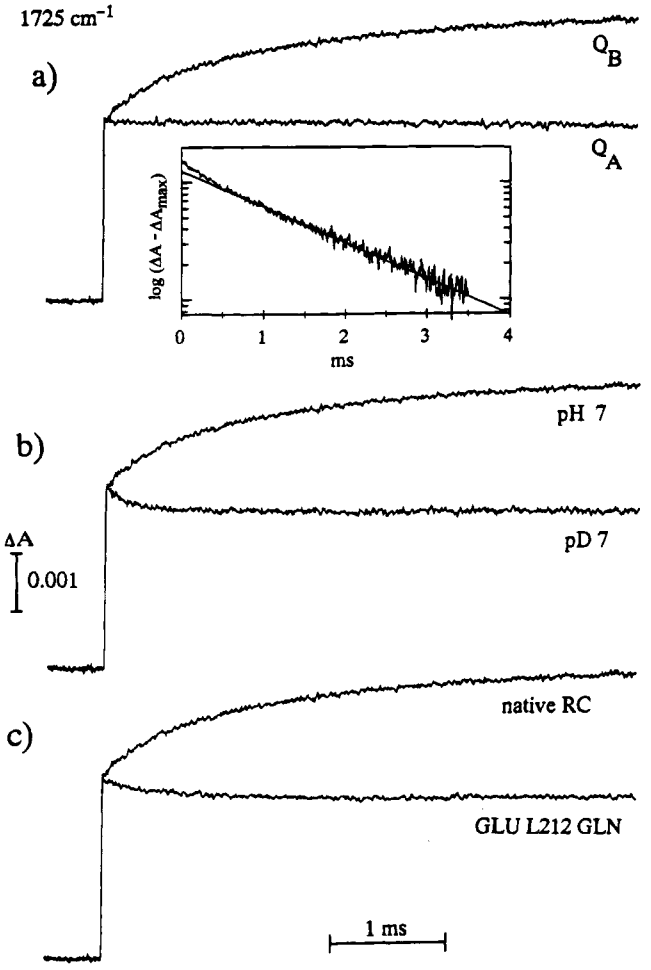

FIGURE 1: (a) Time-resolved IR signal at 1725 cm^{-1} of a native *Rb. sphaeroides* RC sample with Q_B (upper trace) and a terbutryn-treated sample without Q_B (lower trace) at pH = 7. The signals represent raw, uncorrected transients. The sample was excited at $t = 0$ with a 15 ns, ca. 5 mJ, laser flash at 595 nm. 150 kinetic traces were averaged with a dark adaptation time of 20 s between two flashes. $T = 4$ °C. Inset: upper trace in a semilogarithmic plot. (b) Time-resolved IR signal at 1725 cm^{-1} of a native *Rb. sphaeroides* RC sample in ^1H_2O (upper trace) at pH 7 and equilibrated in a ^2H_2O buffer at pD = 7. Measuring conditions were as in panel a. (c) Time-resolved IR signal at 1725 cm^{-1} of a native (upper trace) and a Glu L212 to Gln mutant (lower trace) *Rb. sphaeroides* RC sample at pH 7. Measuring conditions were as in panel a.

RESULTS

Kinetic IR Signals at 1725 cm^{-1}. Figure 1a (upper trace) shows a time-resolved IR signal at 1725 cm^{-1} for a native RC sample at pH 7 and 4 °C containing fully functional Q_B. No correction or subtraction of contributions from the donor side has been performed. A rapid absorbance increase is observed after the flash corresponding to the reaction $DQ_AQ_B \rightarrow D^+Q_A^-Q_B$, which cannot be time-resolved with our present instrument resolution (approximately 500 ns). This immediate rise is followed by a slow biphasic transient (clearly seen in the semilogarithmic plot shown in the inset) with half-times of around 200 μs and 1 ms (for a detailed data analysis, see below), attributed to the reaction $D^+Q_A^-Q_B \rightarrow D^+Q_AQ_B^-$. At a longer time scale, the entire signal decays with a half-time of around 1 s corresponding to the reaction $D^+Q_AQ_B^- \rightarrow DQ_AQ_B$ (data not shown). In a terbutryn-treated sample where Q_A is the terminal electron acceptor, the transient millisecond signal is lacking (Figure 1a, lower trace), and the initial non-resolved rise decays with a half-time of around 60 ms corresponding to $D^+Q_A^- \rightarrow DQ_A$ (data not shown). The rapid, non-resolved phase of the signal can thus be associated with charge separation between D and Q_A, which occurs with a half-time of 200 ps (Parson, 1982). The time course of the millisecond transient present with Q_B as a terminal electron acceptor (Figure 1a) matches those previously observed in the spectral range around 1620 cm^{-1} and tentatively attributed to the antisymmetric COO^- stretching mode of Asp or Glu residues affected by $Q_A^-Q_B \rightarrow Q_AQ_B^-$ electron transfer (Hienerwadel et al., 1992a). The millisecond transient at 1725 cm^{-1} reported here represents a counterpart for these signals and supports the view of Asp and Glu residues responding to $Q_A^-Q_B \rightarrow Q_AQ_B^-$ electron transfer by protonation/deprotonation reactions.

The transient IR signals at 1725 cm^{-1} for native RC containing a full Q_B complement at pH 7 and for RC equilibrated in ^2H_2O at pD 7 are shown in Figure 1b. The positive biphasic transient signals (approximately 200 μs and 1 ms half-time, respectively) are removed by $^1H-^2H$ exchange and reveal a smaller negative component with approximately 100 μs half-time, which kinetically matches the fast phase of the signals at pD 7 at other wavelengths. We presume that this negative component arises from Q_A^- reoxidation in the course of $Q_A^-Q_B \rightarrow Q_AQ_B^-$ electron transfer and that it is obscured by the strong positive signal at 1725 cm^{-1} in the pH 7 sample (see below).

In order to assign the absorption changes to specific carboxyl residues, the transient IR spectra of RCs with site-specific replacements in the Q_B pocket were measured. In the Glu L212 to Gln mutant RC, the positive transient at 1725 cm^{-1} is absent (Figure 1c). Instead, a small negative signal is seen. Its amplitude is approximately the same as seen in the $^1H-^2H$ replacement; however, its time course is considerably slower. The simplest explanation for these results is that the absorption increase at 1725 cm^{-1} is due to Glu L212.

Kinetic IR Signals between 1695 and 1780 cm^{-1}. The spectral range from 1695 to 1780 cm^{-1} was analyzed for the spectral distribution of transient IR signals for native RC at pH 7 and pD 7 and for the Glu L212 to Gln mutant, with probing IR laser modes spaced between 2 and 5 cm^{-1}. Figure 2a shows a three-dimensional representation of the signals obtained after suppressing the instantaneously rising signal according to the procedure described in Materials and Methods (Data Analysis). Three distinct positive peaks are detected at 1732, 1725, and 1706 cm^{-1}, and two negative signals appear at 1716 and approximately 1698 cm^{-1} (although this frequency might not correspond to the maximum signal amplitude). The major signals at 1732 and 1725 cm^{-1} are well separated by a minimum at 1729 cm^{-1}.

Figure 2b shows the three-dimensional representation of the signals for native RC containing Q_B equilibrated in ^2H_2O at pD = 7 between 1695 and 1780 cm^{-1}. The major band at 1725 cm^{-1} has fully disappeared, instead a sharp trough is seen in this region, while the signals at 1698, 1706, and 1732 cm^{-1} appear essentially unchanged. In addition, a new negative component appears around 1750 cm^{-1}, and two positive signals appear at 1738 and 1721 cm^{-1}, respectively.

The three-dimensional representation of transient signals from Glu L212 to Gln mutant RCs is shown in Figure 2c. As mentioned above, the positive band at 1725 cm^{-1} in native RC disappears upon mutation, instead a negative band with

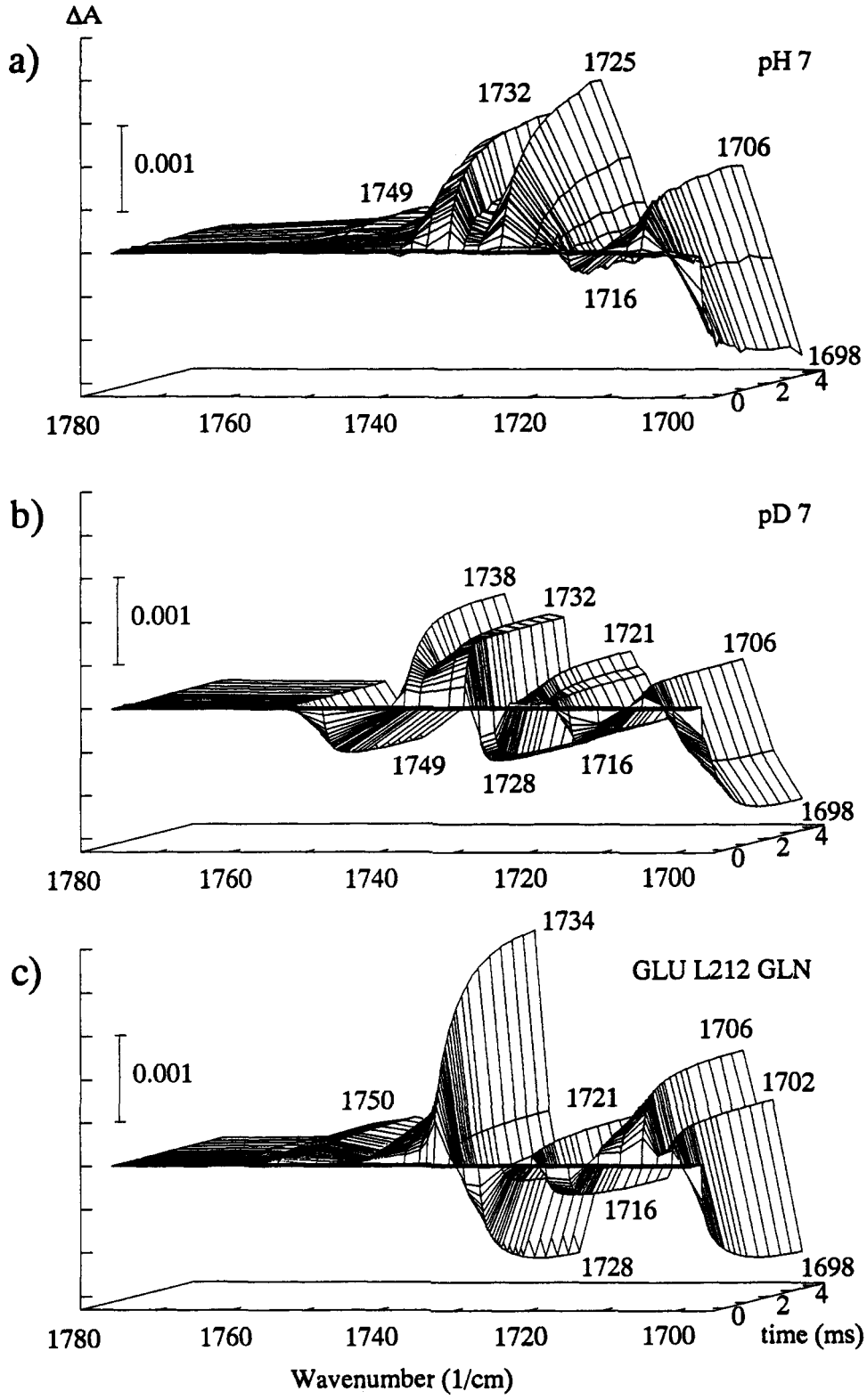

FIGURE 2: Three-dimensional representation of transient IR signals in the 1695−1780 cm^{-1} range for a native *Rb. sphaeroides* RC sample in ^1H_2O at pH 7 (a), a native *Rb. sphaeroides* RC sample equilibrated in ^2H_2O at pD 7 (b), and a Glu L212 to Gln mutant RC sample in ^1H_2O at pH 7 (c). The instantaneously rising component which arises from the $DQ_A \rightarrow D^+Q_A^-$ transition was suppressed (cf. Materials and Methods). The following half-times were calculated from a global fit analysis (for details see text): (a) 0.18 ms (fast), 1.05 ms (slow); (b) 0.11 ms (fast), 0.5 ms (slow); (c) 0.13 ms (fast), 0.8 ms (slow).

maximum at 1728 cm^{-1} and a small positive band at 1721 cm^{-1} appears. Compared to the signals of Figure 1a, these are the only signals that are altered with respect to the native RC, since the positive signals at 1706, 1734 (1732), and 1750 cm^{-1} as well as the negative signals at 1698 and 1716 cm^{-1} remain essentially the same with the exception that the total amplitude of the 1734 cm^{-1} signal is increased.

Kinetic Analysis of the IR Signals. The signals in the 1695−1780 cm^{-1} range were subjected to a global fit analysis using a single set of time constants. A sum of two exponentials was sufficient for a satisfactory fit at all wavelengths, yielding half-times of 1.05 ms and 180 μsec

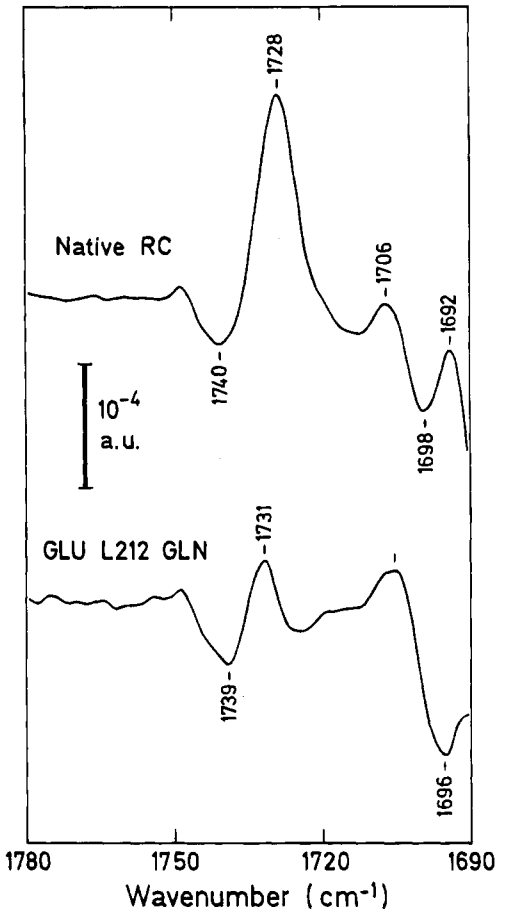

FIGURE 3: Light-induced FTIR difference spectra of Q_B photoreduction for native and Glu L212 Gln mutant RC at pH 7 and 15 °C. Resolution: 4 cm^{-1}; AU: absorbance units.

(for the native sample at 4 °C) with amplitudes varying with wavelength. The quality of the fits was judged from the plot of the weighted residuals, by the statistical χ^2 criterion and from the correlation matrix of the optimized parameters. Analysis for a sum of two exponentials usually resulted in low correlation of the rate constants, residuals distributed randomly around the zero-absorbance line, and a global residual χ^2 value close to 1 [for details on the estimation of the fit quality, cf. Müller et al. (1991)]. The half-times of the fast and slow components as obtained from the global fit are indicated in the legend to the 3-D plots (Figure 2, a-c).

Figure 3 shows FTIR spectra of Q_B photoreduction (Q_B^-/Q_B) in the spectral region between 1780 and 1690 cm^{-1} for native and Glu L212 RC. The main positive peak in the Q_B^-/Q_B difference spectra of the native RC at 1728 cm^{-1} completely disappears for the mutant RC. The negative signals at 1739 and 1698 cm^{-1} as well as the positive signal at 1706 cm^{-1} remain unchanged and experience only minor shifts of the peak maxima.

The spectral distribution of the total signal and of the fast and the slow component of a native RC sample at pH 7, of the RC in ^2H_2O at pD 7, and of a Glu L212 Gln RC sample are shown in Figure 4. The relative amplitudes of the slow and the fast component vary considerably for the different wavelengths. For the major positive signal at 1725 cm^{-1} present in the data for the native RC but absent for RC suspended in ^2H_2O (Figures 1b and 2b) and for Glu L212 Gln RC (Figures 1c and 2c), the slow component dominates (approximately 75% of the total amplitude), whereas the adjacent negative signal at 1716 cm^{-1} exhibits almost exclusively the fast phase.

Dependence of the 1725 cm^{-1} Signal on pH. The amplitude of the 1725 cm^{-1} signal exhibits a distinct dependence on pH. If one assumes that the assignment of this signal to proton uptake by Glu L212 is correct, its amplitude should increase with increasing ionization of Glu L212. Figure 5 shows the amplitude as a function of pH for the total signal at 1725 cm^{-1} and for its fast and slow components as a result of the fit analysis for individual wavelengths. The amplitude of the total signal does not vary significantly between pH 5 and pH 9, except for a "dip" at pH 6. Above pH 9.5, however, the amplitude increases. The slow component decreases from pH 5 to pH 6.3 and then rises continuously up to pH 10. The fast component decreases with rising pH and is almost zero at high pH.

DISCUSSION

The transient IR signals in the microsecond to millisecond time scale studied in this work are attributed to the reaction $Q_A^-Q_B \rightarrow Q_AQ_B^-$. This assignment is based on the absence of these signals in RCs lacking Q_B (e.g., Figure 1a). In samples without Q_B, the only signals observed are the instantaneously rising signals (unresolved with the present time resolution of approximately 500 ns) due to the reaction $DQ_A \rightarrow D^+Q_A^-$ which decay with a half-time of approximately 60 ms ($D^+Q_A^- \rightarrow DQ_A$).[2] Additional support for the assignment of these signals to the $Q_A^-Q_B \rightarrow Q_AQ_B^-$ reaction is that the spectral distribution of the transient IR signals for the native RC (Figure 2a) can be successfully modeled by the sum of the steady-state FTIR spectra for Q_A^- oxidation and Q_B reduction obtained from the Q_B^-/Q_B [Figure 3; see also Breton et al. (1991b) and Bauscher et al. (1993)] and the inverted Q_A^-/Q_A (Mäntele et al., 1990a; Breton et al., 1991a; Bauscher et al., 1993) FTIR difference spectra.

In FTIR difference spectra from the $Q_B \rightarrow Q_B^-$ transition, the main peak in the 1695−1780 cm^{-1} region is an absorbance increase at 1728 cm^{-1} (Figure 3). This peak appears to be responsible for the band in the kinetic IR spectrum at 1725 cm^{-1}. The main features of the $Q_A^- \rightarrow Q_A$ transition are a negative band at 1728 cm^{-1} and a positive band at 1735 cm^{-1} (Mäntele et al., 1990a; Breton et al., 1991a; Bauscher et al, 1993). The modeling of the steady-state difference spectra for $Q_A^-Q_B \rightarrow Q_AQ_B^-$ electron transfer (reoxidation of Q_A and reduction of Q_B) from individually taken Q_B^-/Q_B and Q_A^-/Q_A FTIR difference spectra shows that the main peak at 1728 cm^{-1} in the $Q_B \rightarrow Q_B^-$ transition is shifted to 1725 cm^{-1} in the $Q_A^-Q_B \rightarrow Q_AQ_B^-$ transition. The positive band at 1732 cm^{-1} in the kinetic difference spectra can therefore be attributed partially to a mode from the Q_A site. We therefore state an overall agreement between the kinetic IR data and the FTIR spectra. This agreement is not a necessary requirement since FTIR spectra monitor the fully relaxed state after electron transfer while kinetic IR

[2] In the 1730−1740 cm^{-1} region, small but reproducible signals in the time range of microseconds have been detected even in the complete absence of Q_B (Hienerwadel, 1993). These signals can be associated with the formation of $D^+Q_A^-$ but are much slower than the instantaneously rising components described above associated with Q_A reduction and are also supposed to arise from COOH residues.

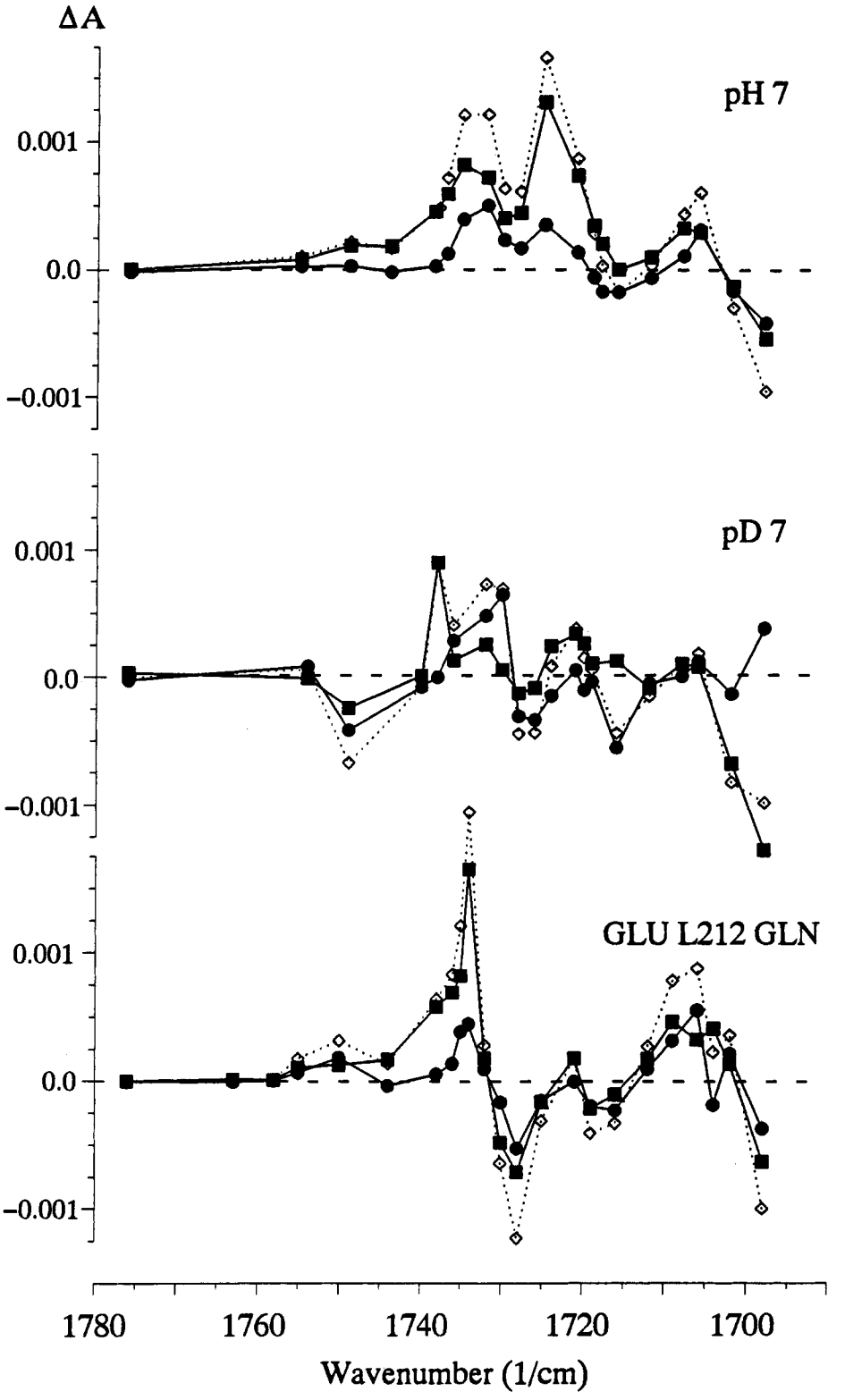

FIGURE 4: Amplitude spectra obtained as a result of a global fit analysis of the signals shown in Figure 2. A single set of two rates was used to calculate the amplitude spectra of the total (open diamonds), the fast (full circles), and the slow (full squares) components. The corresponding half-times are given in the legend to Figure 2.

signals reflect the dynamical change of IR absorbance bands induced by electron transfer. The agreement between the kinetic IR spectra and the sum of the FTIR spectra indicates that the $Q_A^- \rightarrow Q_A$ transition in the presence of Q_B is similar to the relaxed Q_A^-/Q_A transition monitored by FTIR. This indicates that the major spectral change induced by Q_A^- formation, e.g., the band near 1732 cm^{-1} in this work, forms rapidly on the time scale of the kintic IR mesurements (<500 ns).

A straightforward interpretation of the kinetic IR changes in the 1695−1780 cm^{-1} range is that they arise from changes involving COOH residues. In static FTIR investigations of the $Q_A \rightarrow Q_A^-$, $Q_B \rightarrow Q_B^-$, and $D \rightarrow D^+$ transitions, difference bands in this frequency range have been observed

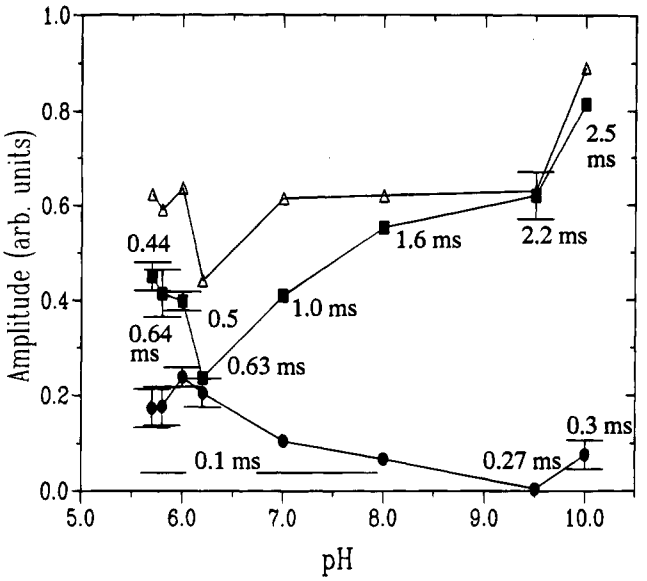

FIGURE 5: Dependence of the signal amplitudes and half-times on pH for a native *Rb. sphaeroides* RC sample at 1725 cm^{-1}. Open diamonds represent the total signal, full circles represent the amplitude of the fast component, and full squares represent that of the slow component. The half-times given at the data points are the result of a single wavenumber fitting analysis and may thus slightly deviate from the half-times of the global fit analysis given in Figure 2. Error bars are given according to the deviations between different measurements and fits. Note that the ordinate is in arbitrary units and not in protons bound.

(Mäntele et al., 1990a; Breton et al., 1991a,b; Leonhard & Mäntele, 1993). In D^+/D difference spectra, the signals in this range could be identified as shifts and intensity changes of the 9-keto and 10a ester C=O modes of the primary donor bacteriochlorophylls. There was no evidence, at least at neutral pH, that changes of protonation of COOH residues occur upon primary donor oxidation (Leonhard & Mäntele, 1993).

In the Q_A^-/Q_A and Q_B^-/Q_B FTIR difference spectra, the signals in the region from 1695 to 1780 cm^{-1} have been proposed to arise from the C=O group of a carboxylic acid side chain residue changing protonation state or from shifts of a COOH residue's C=O mode frequency arising from a change of environment for the $Q_A \rightarrow Q_A^-$ transition (Mäntele et al., 1990; Breton et al., 1991a; Bauscher et al., 1993). The possibility of a small shift of an ester C=O group of BPheo in response to the electric field caused by Q_A reduction, however, has also been considered (Mäntele et al., 1990a; Breton et al., 1992a; Bauscher et al., 1993). Whether an electrochromic shift of an IR band could yield significant contributions to the difference spectra is difficult to estimate, mainly for lack of suitable model systems.

However, the shift of the electronic levels of BPheo in the near-infrared upon Q_A^- formation is very small compared to effects of the BPheo anion formation. In analogy to this, a vibrational electrochromic shift, if present at all, would represent a very minor effect with respect to the substantial changes in the IR spectrum upon anion formation. With this in mind, the most probable interpretation is that the time-resolved IR signals in the 1695−1780 cm^{-1} range can be associated with changes at Asp or Glu side chains, representing changes either of protonation or of the local environment of residues that are already protonated in the dark-adapted state of the sample. If this is correct, it then follows that the Q_A^-/Q_A difference spectrum in this range is mainly caused by Asp/Glu residues.

On the other hand, the main kinetic IR signals in the frequency range of approximately 1695−1760 cm^{-1} exhibit a strong dependence on external pH not only for their half-times but also for their amplitudes (Hienerwadel, 1993). This leads us to the conclusion that, in case a pheophytin shift should contribute to the kinetic IR difference spectra, this shift would not only be affected by electron transfer but also by electrostatic rearrangement due to proton transfer.

Assignment of the 1725 cm^{-1} Signal to Proton Uptake by a Carboxylate Residue, Most Probably to That of Glu L212. The most prominent feature of the kinetic IR spectrum is the peak at 1725 cm^{-1}. The assignment of this peak to the COOH group of Glu L212 is based on its spectral position in the COOH region, its loss upon $^1H_2O \rightarrow {}^2H_2O$ exchange, and its absence in Glu L212 to Gln RCs. The signal at 1725 cm^{-1} in native RC (Figure 1a) could be due to the uptake of a proton by an ionized COO^- group or to the shift of an already protonated COOH group. We assign the large absorption increase due to the 1 ms component at 1725 cm^{-1} to proton uptake ($H^+ + COO^- \rightarrow COOH$); this component is not likely to arise from the shift of an existing COOH band in view of the absence of a corresponding negative band (Figure 4). This is clearly confirmed by the steady-state Q_B^-/Q_B difference spectra for native RC and for the Glu L212 Gln mutant (Figure 3). The negative band below 1700 cm^{-1} cannot be the negative counterpart of the 1725 cm^{-1} signal (1728 cm^{-1} in the steady-state Q_B^-/Q_B FTIR spectra) since it is unchanged by deuteration or Glu L212 to Gln mutation (Figures 2 and 3). However, the 100 μs component at 1725 cm^{-1} could result from the shift of an existing COOH band. The corresponding negative counterpart could be the negative band at 1716 cm^{-1} (Figure 4) or a small negative component at another frequency masked by a positive increase due to a different group.

Protonated Asp and Glu side chain residues in model compounds (Venyaminov & Kalnin, 1990) or in a protein (Siebert et al., 1982) can show a distinct impact of $^1H-{}^2H$ exchange on the C=O mode. In model compounds, this corresponds to a 5−10 cm^{-1} shift to a lower frequency (Venyaminov & Kalnin, 1990). This shift is caused by uncoupling of the $O-{}^1H$ ($O-{}^2H$) mode from the C−O mode in the COO^2H group (Bellamy, 1966). The sensitivity of a vibrational mode in the range analyzed here to $^1H \rightarrow {}^2H$ exchange can thus be used as a simple tool for identification of a COOH group, implying that the residue is fully accessible and the $^1H \rightarrow {}^2H$ exchange can proceed. Ideally, a peak of the COO^1H mode should have a matching peak of the COO^2H mode downshifted by 5−10 cm^{-1}. However, additional influence of the p*K* shift in ^2H_2O, in particular for several interacting ionizable residues, could reduce the amplitude of the shifted peak. Thus, the primary argument taken from a $^1H_2O/{}^2H_2O$ effect should be the absence of a peak in ^2H_2O, and the absence of a shifted band does not necessarily exclude the assignment of the signal to carboxylic groups. Both the formation of a COOH group by proton uptake and the shift of an existing COOH group by a change of the environment should manifest the same way.

The decrease of the strong positive 1725 cm^{-1} signal in RCs equilibrated in ^2H_2O (Figure 2b) provides evidence for the assignment of the signal to a COOH band. The small positive signal around 1721 cm^{-1} could be the corresponding

COO^2H band. The lower amplitude of this band could be due to a lower $^2H^+$ uptake in ^2H_2O caused by an increase in the pK of the COO^2H group. Evidence for a change of pK in ^2H_2O comes from the additional signal components at 1738 and 1749 cm^{-1}.

The simplest interpretation of the absence of the 1725 cm^{-1} signal in Glu L212 Gln RCs is that the signal is due to the COOH mode of Glu L212. This assignment is consistent with the assignment made from the FTIR measurements shown in Figure 3 for native and Glu L212 Gln RC and for the Asp 213 Asn mutant (Hienerwadel et al., 1992b). An alternative explanation for the result is that the Glu L212 to Gln change results in the modification of the pK_a of a second COOH group, which is responsible for the 1725 cm^{-1} signal either by a change in conformational or electrostatic interaction. The conformational change is not likely since the crystal structure of the mutant RC is not appreciably different from that of native RCs (Chirino et al., 1994). The electrostatic interaction would be consistent with the prediction by Gunner and Honig (1992) that Glu L212 is fully ionized. However, it is not consistent with the earlier assignment of a high pK_a (9.5) to Glu L212. Additionally, the two most likely candidates for the second residue, Asp L213 and Asp L210, can be ruled out since their mutation does not eliminate the 1725 cm^{-1} signal (Hienerwadel et al., 1992b, 1993), making this alternative unlikely.

Figure 2c shows the three-dimensional representation of the signals from the Glu L212 to Gln mutant in ^1H_2O at pH 7 with a full Q_B complement. The main modifications of the difference spectrum are the disappearance of the 1725 cm^{-1} band, an increase of the amplitude of the 1734 cm^{-1} signal (at 1732 cm^{-1} for the native RC), a new negative signal at 1728 cm^{-1}, and a new positive band at 1702 cm^{-1}. Mutation of a charged to a neutral residue might lead to a distortion of the electrostatic interactions in the binding site and might thus cause additional signals or modify signals of remaining groups. The residual structure of the time-resolved difference spectrum however remains unchanged. As discussed above, these signals may partly be associated with the $Q_A \rightarrow Q_A^-$ transition. The possibility that the 1 ms component of the 1725 cm^{-1} signal in native RCs shifts either to 1734 or 1702 cm^{-1} in the mutant with an additional decrease in the pK of the observed group due to the mutation seems rather unlikely. This would require an electrostatic interaction with an ionized Glu L212 at pH 7 and should give rise to a pH-dependent shift of the 1725 cm^{-1} band in native RCs. Neither the pH dependence of the 1725 cm^{-1} signal (see Figure 4) nor the global fit analysis of the signals in the 1695−1780 cm^{-1} region for low and high pH (Hienerwadel, 1993) indicate a shift for this band. We therefore suggest that the signals at 1734 cm^{-1} and around 1706 cm^{-1} in the steady-state Q_B^-/Q_B FTIR difference spectra of the Glu L212 Gln mutant are due to compensating proton uptake of other Asp or Glu side chains. The existence of compensating groups for Glu L212 and Asp L213 in *Rhodobacter capsulatus* RC has been proposed by Schiffer et al. (1992).

The non-ionizable residue Gln L212 in the Glu L212 Gln mutant should not give rise to any IR signal directly associated with the fractional protonation of groups forming the Q_B site. However, the Gln C=O mode, which is located at 1670−1680 cm^{-1} in model compounds (Venyaminov & Kalnin, 1990), might respond to microconformational or electrostatic changes brought about by protonation or deprotonation of other residues. At present, however, we have no evidence for a differential band arising from the Gln C=O mode at the lower limit of our kinetic spectra. A comparative FTIR study of native RC and mutants in the frequency range from 1800 to 1000 cm^{-1} is currently under progress.

The balance of evidence favors an assignment of the 1725 cm^{-1} signal to (partial) proton uptake of Glu L212 in consequence of formation of Q_B^-. In order to analyze whether formation of Q_A^- has some impact on this residue, we have compared the signal amplitudes at $t = 5$ μs between 1695 and 1780 cm^{-1} for native and Glu L212 Gln mutant RCs at pH 7 (data not shown). The signal amplitudes only differ significantly at 1738 cm^{-1}. We thus conclude that Glu L212 is ionized prior to the flash and does not change its protonation state upon formation of Q_A^-. The signal change at 1738 cm^{-1} can be attributed to an electrostatic influence of ionized Glu L212 on another group, since the signal is not only caused by the Glu L212 to Gln mutation but also by a Glu L104 to Leu mutation [data not shown; cf. Hienerwadel (1993)].[3] These signal changes are interpreted as a clear indication that the electrostatic influence of ionized Glu L212 has a long-range action within the protein.

The peak position of the 1728 cm^{-1} band in the steady-state FTIR difference spectra, which we assume to arise from proton uptake by Glu L212, does not differ significantly from that found in model systems such as Asp or Glu in suitable buffers (Venyaminov & Kalnin, 1990). On the other hand, in bacteriorhodopsin the highest frequency found for such residues is at 1762 cm^{-1} [for references, see Rothschild (1992)] and was taken as an argument for a strictly aprotic environment for the respective residue. If our assignment of the 1728 cm^{-1} is correct, we conclude that the microenvironment for Glu L212 is reasonably "aqueous", in a sense that it could be in interaction with several water molecules. In fact, calculations (Beroza et al., 1992) as well as a higher-resolution X-ray structure (Ermler et al., 1994) predict water molecules in the Q_B environment. In addition, there is no indication for another carboxylic acid group that could serve as a proton donor to Glu L212. This observation would support a model of a water channel from the outside of the protein to the Q_B pocket.

Origin of the Fast and Slow Phases. The 1725 cm^{-1} signal tentatively assigned to Glu L212 as well as other signals in the 1695−1750 cm^{-1} range display two kinetic phases. A working model to explain the biphasic kinetics in native RCs is that the fast step involves electron transfer from Q_A^- to Q_B in RC in which Glu L212 is protonated (4a) while the slow step involves a combination of electron and proton transfer to RC in which Glu L212 is ionized (4b). This interpretation is consistent with the assignment of the slow phase of the 1725 cm^{-1} signal to a new COOH mode resulting from proton uptake and the fast phase to a shift of a COOH mode of an existing protonated acid.

$$\underset{HA}{Q_A^-Q_B} \xrightarrow{\tau\ \text{fast}} \underset{HA}{Q_AQ_B^-} \qquad (4a)$$

[3] RCs with Glu L104 replaced by Leu were a generous gift from J. Allen (Arizona State University, Tempe, AZ).

$$H^+ + \underset{A^-}{Q_A{}^-Q_B} \xrightarrow{\tau\ \text{slow}} \underset{HA}{Q_AQ_B{}^-} \quad (4b)$$

In this model, HA for the fast phase may be identified either with a fractionally protonated Glu L212 or with other Asp/Glu residues in the Q_B site, and A^- or HA for the slow phase may be identified with Glu L212. The slow rate could be due to rate-limiting proton uptake before electron transfer or rate-limiting electron transfer with A^- present followed by proton transfer. It should be noted, however, that the proton uptake associated with the slow phase does not necessarily imply full protonation.

A second model which explains the biphasic kinetics is that the two states in eq 4 involve different conformational states of the RC, either near Q_A or Q_B. In this model, the two rates would result from different electron transfer rates in the two conformations or by the rate of transition from an inactive conformation to an active one followed by electron transfer. This model would be consistent with the observation of biphasic rates in Glu L212 to Gln RCs. Conformational changes due to Q_A reduction have been invoked to explain electrogenic transients (Brzezinski et al., 1992), proton uptake (Wraight & Maroti, 1990), and electrochromic shifts (Tiede & Hanson, 1992). A third model is that electron transfer between quinones is not a single electron transfer step but involves a transient redox intermediate (Paddock et al., 1994b). In this case, the biphasic rate would be due to two electron transfer steps in series.

The biphasic kinetics reported here are consistent with the reported biphasic $Q_B \rightarrow Q_B{}^-$ reaction monitored at the C−O mode of $Q_B{}^-$ at 1478 cm^{-1}, which displays 200 μs and 1 ms components at pH 7 and 4 °C (Hienerwadel, 1993; Hienerwadel et al., 1994). On the other hand, optical measurements on the same sample at 760 nm (data not shown) show only a 1 ms phase in agreement with previous measurements of the change at 760 nm at 4 °C (Mancino et al., 1984). We conclude from this that the absorbance changes monitored at 760 nm respond mainly to proton transfer or to conformational changes of the protein. This is consistent with results of Tiede and Hanson (1992), who reported that absorbance changes in the 700−900 nm region in chromatophores from *Rb. capsulatus* were sensitive to protein relaxation. The detailed kinetics of electron and proton transfer reactions in the RC as monitored at specific IR vibrational modes of the quinones will be described in more detail in a later publication.

Estimation of H^+/e^- Stoichiometry. Extinction coefficients for the C=O bond of protonated Glu residues have been measured to be around 200−300 L mol^{-1} for isolated amino acids (Venyaminov & Kalnin, 1990). There is, however, considerable uncertainty on the molar extinction coefficient of this mode *in situ*. For an estimation of the H^+/e^- stoichiometry, we have to consider the different half-widths of the COOH modes, which is approximately 50 cm^{-1} for the isolated amino acid (Venyaminov & Kalnin, 1990), indicating conformational flexibility, but only 8−10 cm^{-1} for the difference band at 1725 cm^{-1}. If we take into account these integrated extinction coefficients, we can roughly estimate that the 1 ms transient at 1725 cm^{-1} arises from uptake of 0.3−0.6 protons per RC at pH 7. Based on this result, we propose that the proton uptake by Glu L212 near pH 7 can account for a large part of the measured total proton uptake of approximately 0.4 H^+/e^- at pH 7 (McPherson et al., 1988; Shinkarev et al., 1993). McPherson et al. (1994) have observed that the proton uptake due to the mutation Glu L212 to Gln is not changed near pH 7 but is significantly reduced at higher pH (by 0.2 H^+/e^- at pH 8.5). This indicates that compensating proton uptake by other residues must occur in the mutant near pH 7. Such compensating changes in protonation may be indicated by absorbance increase in the kinetic IR spectrum of the Glu L212 to Gln mutant in the carboxyl region, e.g., the peak at 1734 cm^{-1} (see Figure 2c). An alternative interpretation for the increase of the 1734 cm^{-1} band in the mutant could be the presence of contributions from $Q_A{}^-$ reoxidation. A thorough analysis of the ratio of the fast (180 μs) and slow (1.05 ms) components within the band profile should help to settle this question.

The IR signal at 1725 cm^{-1} has a half-width of less than 10 cm^{-1}. This is considerably less than the half-width of approximately 50 cm^{-1} observed for the COOH mode of Asp or Glu residues in aqueous buffers (Venyaminov & Kalnin, 1990). In a recent analysis of the redox reaction of halocyanin, a small type I copper protein, protonation of an Asp/Glu residue concomitant with oxidation was found at low pH (Brischwein et al., 1993). The half-width of this COOH mode was >50 cm^{-1}, as expected for a solvated residue at the surface of the protein, with full rotational freedom and fully accessible to the aqueous phase. The relatively sharp band at 1725 cm^{-1} is consistent with a fixed position and restricted rotational freedom for the Glu L212 group in the RC. These steric constraints may explain the large difference in proton and electron transfer between RCs with Glu and Asp at position L212 (Paddock et al., 1990b).

pH Dependence of the 1725 cm^{-1} Signal. The proton uptake of the carboxylate residue, assigned here to Glu L212, is assumed in our model to be proportional to the amplitude of the slow kinetic component of the 1725 cm^{-1} signal. It is relatively pH independent, increasing gradually by 0.2−0.3 H^+ in the range from pH 5 to pH 10, with an increase at pH $\geq 10^4$ (see Figure 5). If the assignment is correct, this agrees with a gradually increasing ionized fraction of Glu L212. The amplitude of the fast kinetic component decreases with increasing pH. This is consistent with the assignment of this component to the protonated form of Glu L212 which decreases at high pH. The variation of proton uptake (slow component) by Glu L212 with pH is inconsistent with qualitative estimates obtained from a simple model in which Glu L212 has a pK_a of 9.5 in the Q_B state increased to ≈11 in the $Q_B{}^-$ state (Paddock et al., 1989; Takahashi & Wraight, 1992). In such a model, the proton uptake would be small at low pH (<0.01 H^+/RC at pH 7) with a maximum above pH 9.5 (McPherson et al., 1988).

The pH dependence of the protonation of Glu L212 is clearly different from that expected from the Henderson−Hasselbalch relation for single isolated titrating residues. A possible explanation for this result is that the pH is not reliably determined in the concentrated IR sample because of buffering groups at the protein. However, similar IR titrations on other proteins have been shown to give good

[4] The proton uptake is uncorrected for the equilibrium between $Q_A{}^-Q_B \rightleftharpoons Q_AQ_B{}^-$, which is less favorable to Q_B at pH >9 (Kleinfeld et al., 1984). Thus, the increase in proton uptake (H^+/e^-) at high pH should be even greater. This large increase in proton uptake might explain the inflection point in K_{BD} vs pH at pH 9.5.

agreement with solution results (Brischwein et al., 1993). In addition, the pH dependence of k_{BD} (Kleinfeld et al, 1984) measured in the RC samples was used to calibrate pH in the lower range. Another possible explanation for the difference is that the proton uptake may be due to the sum of the amplitudes of the slow and fast components which is almost constant over the full titration range. This would be expected if the pK_a of Glu L212 were <5 with Q_B^- present. However, this interpretation is inconsistent with the low stoichiometry (H^+/RC < 1.0) and with the increased proton uptake at high pH.

The observed proton uptake can be accounted for by considering interactions between titrating residues as emphasized by recent electrostatic calculations (Beroza et al., 1991; Gunner & Honig, 1992; Beroza, 1993). Gunner and Honig (1992) have calculated that Glu L212 should pick up $1H^+/Q_B^-$ over most of the pH range decreasing at high pH. This calculation is consistent with the weak pH dependence; however, the predicted decrease in proton uptake at high pH is inconsistent with the increase at high pH in Figure 5. Beroza (1993) has calculated a gradually increasing proton uptake by Glu L212 with pH in agreement with the measured values presented here. The differences between the calculations may be attributed to differences in the parameters used by the different groups (Beroza et al., 1994). However, it is clear both from calculations and experiments that Glu L212 interacts strongly with other titrating residues. These interactions are attributed to the low dielectric constant in the interior of the RC near Q_B and the presence of nearby groups with similar pK_a's. These conditions may be features important for proton transfer as pointed out by Bashford and Gerwert (1992), who observed similar interactions in bacteriorhodopsin.

CONCLUSIONS

Time-resolved IR and steady-state FTIR spectroscopy have provided strong evidence that Glu L212 is involved in proton uptake stabilizing Q_B^-. This protonation may be understood in a simple way as providing charge compensation for the state Q_B^- and along with protonation or deprotonation of other ionizable residues forming a *variable electrostatic reaction field* around Q_B which balances the excess negative charge on Q_B^-. The involvement of other residues is reflected in changes in the kinetic IR spectrum in the 1698–1770 cm^{-1} region.

The interactions between other titrating residues and that observed at 1725 cm^{-1}, which is proposed to be Glu L212, would give rise to a complex titration behavior of the Glu L212 proton uptake. This behavior may be a common feature in other proton transfer proteins. Further identification of interacting residues using both kinetic IR and FTIR spectroscopy is currently in progress and involves measurements on mutant RCs at different pH values (Nabedryk et al., 1993) and double-flash experiments. The combination of both techniques will allow specific investigations of single protonatable residues under various conditions. Such studies should help to elucidate the mechanism of proton transport in bacterial reaction centers.

ACKNOWLEDGMENT

The authors would like to thank Prof. G. Feher (UCSD) and Dr. M. Bauscher (Institut für Biophysik) for valuable discussions and E. Abresch (UCSD) for preparation of mutant RC. A gift of *Rb. sphaeroides* Glu L104 to Leu mutant RCs from Prof. J. Allen (Arizona State University, Tempe, AZ) is greatly appreciated. We thank Dr. P. Beroza (UCSD) and Prof. M. Gunner (City College of New York) for stimulating discussions on protein electrostatics and appreciate generous help from Dr. K. H. Müller (MPI Dortmund), who provided us with the Mexfit program.

REFERENCES

Allen, J. P., Feher, G., Yeates, T. O., Rees, D. C., Deisenhofer, J., Michel, H., & Huber, R. (1986) *Proc. Natl. Acad. Sci. U.S.A. 83*, 8589–8593.

Allen, J. P., Feher, G., Yeates, T. O., Komiya, H., & Rees, D. C. (1987) *Proc. Natl. Acad. Sci. U.S.A. 84*, 6162–6166.

Bagley, K. A., Abresch, E., Okamura, M. Y., Feher, G., Bauscher, M., Mäntele, W., Nabedryk, E., & Breton, J. (1990) in *Current Research in Photosynthesis* (Baltscheffsky, M., Ed.) Vol. I, pp 77–80, Kluwer Academic Publishers, Dordrecht, The Netherlands.

Bashford, D., & Gerwert, K. (1992) *J. Mol. Biol. 224*, 473–486.

Bauscher, M., & Mäntele, W. (1992) *J. Phys. Chem. 96*, 11101–11108.

Bauscher, M., Nabedryk, E., Bagley, K. A., Breton, J., & Mäntele, W. (1990) *FEBS Lett 261*, 191–195.

Bauscher, M., Leonhard, M., Moss, D. A., & Mäntele, W. (1993) *Biochim. Biophys. Acta 1183*, 59–71.

Bellamy, L. J. (1966) *Ultrarotspektrum und Chemische Konstitution*, (Steinkopff, D., Ed.) Verlag, Darmstadt, Germany.

Beroza, P. (1993) Ph.D. Thesis, Department of Physics, University of California, San Diego, La Jolla, CA.

Beroza, P., Fredkin, D. R., Okamura, M. Y., & Feher, G. (1991) *Proc. Natl. Acad. Sci. U.S.A. 88*, 5804–5808.

Beroza, P., Fredkin, D. R., Okamura, M. Y., & Feher, G. (1994) *Biophys. J. 66*, A229.

Breton, J., Thibodeau, D. L., Berthomieu, C., Mäntele, W., Verméglio, A., & Nabedryk, E. (1991a) *FEBS Lett. 278*, 257–260.

Breton, J., Berthomieu, C., Thibodeau, D. L., & Nabedryk, E. (1991b) *FEBS Lett. 288*, 109–113.

Breton, J., Burie, J.-R., Berthomieu, C., Thibodeau, D. L., Andrianambinintsoa, S., Dejonghe, D., Berger, G., & Nabedryk, E. (1992a) in *The Photosynthetic Bacterial Reaction Center II* (Breton, J., & Verméglio, A., Eds.) pp 155–162, Plenum Press, New York.

Breton, J., Nabedryk, E., & Parson, W. W. (1992b) *Biochemistry 31*, 7503–7510.

Breton, J., Burie, J.-R., Berthomieu, C., Berger, G., & Nabedryk, E. (1994) *Biochemistry 33*, 4953–4965.

Brischwein, M., Scharf, B., Engelhard, M., & Mäntele, W. (1993) *Biochemistry 32*, 13710–13717.

Buchanan, S., Michel, H., & Gerwert, K. (1992) *Biochemistry 31*, 1314–1321.

Chang, C. H., Tiede, D. M., Tang, J., Norris, J., & Schiffer, M. (1986) *FEBS Lett. 205*, 82–86.

Chirino, A. J., Lous, E. J., Huber, M., Allen, J. P., Schenck, C. C., Paddock, M. L., Fehr, G., & Rees, D. C. (1994) *Biochemistry 33*, 4584–4593.

Cramer, W. A., & Knaff, D. B. (1990) *Energy Transduction in Biological Membranes*, Springer Verlag, New York.

Deisenhofer, J., Epp, O., Miki, K., Huber, R., & Michel, H. (1984) *J. Mol. Biol. 180*, 385–398.

El-Kabbani, O., Chang, C. H., Tiede, D. M., Norris, J., & Schiffer, M. (1991) *Biochemistry 30*, 5361–5369.

Ermler, U., Fritzsch, G., Buchanan, S. K., & Michel, H. (1994) *Structure 2*, 925–936.

Feher, G., Isaacson, R. A., Okamura, M. Y., & Lubitz, W. (1985) in *Antennas and Reaction Centers of Photosynthetic Bacteria* (Michel-Beyerle, M. E., Ed.) pp 174–189, Springer Verlag, Berlin.

Gunner, M., & Honig, B. (1992) in *The Photosynthetic Bacterial Reaction Center II* (Breton, J., & Verméglio, A., Eds.) pp 403–410, Plenum Press, New York.

Hienerwadel, R. (1993) Ph.D. Thesis, Department of Chemistry, University of Freiburg, Freiburg, Germany.
Hienerwadel, R., Thibodeau, D. L., Lenz, F., Nabedryk, E., Breton, J., Kreutz, W., & Mäntele, W. (1992a) *Biochemistry 31*, 5799−5808.
Hienerwadel, R., Nabedryk, E., Paddock, M. L., Rongey, S., Okamura, M. Y., Mäntele, W., & Breton, J. (1992b) in *Research in Photosynthesis* (Murata, M., Ed.) Vol. I, pp 437−440, Kluwer Academic Publishers, Dordrecht, The Netherlands.
Hienerwadel, R., Fogel, C., Grzybek, S., & Mäntele, W. (1994) *Biophys. J. 66*, A365.
Kleinfeld, D., Okamura, M. Y., & Feher, G. (1984) *Biochim. Biophys. Acta 766*, 126−140.
Leonhard, M., & Mäntele, W. (1993) *Biochemistry 32*, 4532−4538.
Lubitz, W., Abresch, E. C., Debus, R. J., Isaacson, R. A., Okamura, M. Y., & Feher, G. (1985) *Biochim. Biophys. Acta 808*, 464−469.
Mancino, L. J., Dean, D. P., & Blankenship, R. E. (1984) *Biochim. Biophys. Acta 764*, 46−54.
Mäntele, W. (1993) Infrared spectroscopy of the photosynthetic reaction center, in *The Photosynthetic Bacterial Reaction Center* (Deisenhofer, J., & Norris, J., Eds.) Volume II, Chapter A10, pp 239−283, Academic Press, New York.
Mäntele, W., Nabedryk, E., Tavitian, B. A., Krewutz, W., & Breton, J. (1985) *FEBS Lett. 187*, 227−232.
Mäntele, W., Leonhard, M., Bauscher, M., Nabedryk, E., Breton, J., & Moss, D. A. (1990a) in *Reaction Centers of Photosynthetic Bacteria; Structure and Dynamics* (Michel-Beyerle, M. E., Ed.) Springer Series in Biophysics 6, pp 31−44, Springer, Berlin.
Mäntele, W., Hienerwadel, R., Lenz, F., Riedel, W. J., Grisar, R., & Tacke, M. (1990b) *Spectrosc. Int. 2*, 29−35.
Maroti, P., & Wraight, C. A. (1988) *Biochim. Biophys. Acta 934*, 329−347.
McPherson, P. H., Okamura, M. Y., & Feher, G. (1988) *Biochim. Biophys. Acta 934*, 348−368.
McPherson, P. H., Schönfeld, M., Paddock, M. L., Okamura, M. Y., and Feher, G. (1994) *Biochemistry 33*, 1181−1193.
Müller, K. H., & Plesser, Th. (1991) *Eur. Biophys. J. 19*, 231−240.
Nabedryk, E., Mäntele, W., Tavitian, B. A., & Breton, J. (1986) *Photochem. Photobiol. 43*, 461−465.
Nabedryk, E., Bagley, K. A., Thibodeau, D. L., Bauscher, M., Mäntele, W., & Breton, J. (1990) *FEBS Lett. 266*, 59−62.
Nabedryk, E., Breton, J., Hienerwadel, R., Mäntele, W., Paddock, M. L., Rongey, S. H., Feher, G., & Okamura, M. Y. (1993) *Biophys. J. 64*, A214, 468.
Okamura, M. Y., & Feher, G. (1992) *Annu. Rev. Biochem. 61*, 861−896.
Okamura, M. Y., Isaacson, R. A., & Feher, G. (1975) *Biochim. Biophys. Acta 72*, 3491−3495.
Paddock, M. L., Rongey S. H., Feher, G., & Okamura, M. Y. (1989) *Proc. Natl. Acad. Sci. U.S.A. 86*, 6602−6606.
Paddock, M. L., McPherson, P. H., Feher, G., & Okamura, M. Y. (1990a) *Proc. Natl. Acad. Sci. U.S.A. 87*, 6803−6807.
Paddock, M. L., Okamura, M. Y., & Feher, G. (1990b) *Biophys. J. 57*, 569a.
Paddock, M. L., Rongey, S. H., McPherson, P. H., Juth, A., Feher, G., & Okamura, M. Y. (1994a) *Biochemistry 33*, 734−745.
Paddock, M. L., Graige, M. S., Feher, G., & Okamura, M. Y. (1994b) *Biophys. J. 66*, 127a.
Parson, W. W. (1982) *Annu. Rev. Biophys. Bioeng. 11*, 57−80.
Rongey, S. H., Paddock, M. L., McPherson, P. H., Feher, G., & Okamura, M. Y. (1990) *Biophys. J. 59*, A142.
Rothschild, K. J. (1992) *J. Bioenerg. Biomembr. 24*, 147−167.
Schiffer, M., Chan, C.-K., Chang, C.-H., DiMagno, T. J., Fleming, G. R., Nance, S., Norris, J. R., Snyder, S., Thurnauer, M., Tiede, D. M., & Hanson, D. K. (1992) in *The Photosynthetic Bacterial Reaction Center* II (Breton, J., & Verméglio, A., Eds.) pp 351−361, Plenum Press, New York.
Siebert, F., Mäntele, W., & Kreutz, W. (1982) *FEBS Lett. 141*, 82−87.
Takahashi, E., & Wraight, C. A. (1990) *Biochim. Biophys. Acta 1020*, 107−111.
Takahashi, E., & Wraight, C. A. (1992) *Biochemistry 31*, 855−866.
Thibodeau, D. L., Nabedryk, E., Hienerwadel, R., Lenz, F., Mäntele, W., & Breton, J. (1990) *Biochim. Biophys. Acta 1020*, 253−259.
Thibodeau, D. L., Nabedryk, E., Hienerwadel, R., Lenz, F., Mäntele, W., & Breton, J. (1992) in *Time-Resolved Vibrational Spectroscopy V* (Takahashi, H., Ed.) Springer Proceedings in Physics, Vol. 68, pp 79−82, Springer Verlag, Berlin.
Tiede, D. M., & Hanson, D. K. (1992) in *The Photosynthetic Bacterial Reaction Center II* (Breton, J., & Verméglio, A., Eds.) pp 341−350, Plenum Press, New York.
Venyaminov, S. Y., & Kalnin, N. N. (1990) *Biopolymers 30*, 1243−1257.
Vermeglio, A. (1977) *Biochim. Biophys. Acta 459*, 516−524.
Verméglio, A., & Clayton, R. K. (1977) *Biochim. Biophys. Acta 461*, 159−165.
Wraight, C. A. (1977) *Biochim. Biophys. Acta 459*, 525−531.
Wraight, C. A. (1979) *Biochim. Biophys. Acta 548*, 309−327.

BI940966L